Original Article

Institution of MECHANICAL ENGINEERS

Journal of AUTOMOBILE ENGINEERING

Proc IMechE Part D:
J Automobile Engineering
1–12

DOI: 10.1177/0954407017707670
journals.sagepub.com/home/pid

SAGE

Experimental vibro-acoustic analysis of the gear rattle induced by multi-harmonic excitation

Renato Brancati[1], Ernesto Rocca[1], Daniela Siano[2] and Massimo Viscardi[1]

Abstract

The paper reports a wide vibro-acoustic experimental investigation of the gear rattle phenomenon induced by multi-harmonic excitation. The analysis is performed by using different measurement techniques which allow some of the significant parameters in this type of investigation to be acquired on a specific test rig: the angular rotations of the gears by using encoders; the accelerations obtained from a triaxial accelerometer; the sound pressure level determined by employing both acoustic microphones; the correct evaluation of the acoustic sources by utilizing a *p–v* sound intensity probe. Performance indices were adopted to compare the dynamic behaviours of the system with respect to some parameters, such as the speed of the pinion, the fluctuations in the speed of the pinion and the lubrication conditions. The results of the comparative analysis show very good agreement between the vibro-acoustic measurements and the results from the encoder-based method; this has helped us to interpret the physical behaviour of the gear pair with respect to the impacts occurring between the teeth during the different phases of the phenomenon. Moreover, the study indicates interesting aspects of the effects of multi-harmonic excitation on the rattle phenomenon, with particular attention to the influence of lubrication on the reduction in the rattle noise.

Keywords

Gear rattle, noise, vibration, acoustic measurements

Date received: 27 July 2016; accepted: 14 March 2017

Introduction

Gear rattle is a typical vibro-acoustic phenomenon of the automotive gearbox; it represents today an annoying problem for the car industry with regard to the acoustic comfort and therefore is strictly related to the quality of the product.[1–3]

Gear rattle is caused by fluctuations in the torque of the alternative engine; these produce consequent speed fluctuations which cause repetitive impacts between the teeth of unloaded gear pairs in the gearbox.[1,2] The frequency of these speed fluctuations at the primary shaft of the gearbox depends on the number of cylinders and on the engine technology.[4,5] As an example, in a four-stroke four-cylinder engine, the ignition frequency, which is double that of the rotation frequency, characterizes the rattle cycle. More precisely, because of the discontinuous combustion in the engine, the excitation of the input shaft is of the periodic type with a fundamental frequency which is the same as that of the ignition.

This research topic has been mainly studied by theoretical and experimental approaches, and various methodologies have been adopted. Many theoretical studies deal with the torsional analysis of the entire driveline to reduce the rattle noise by design modifications. In the experimental field, the investigations often consist in analysing a specific automotive gearbox, which is monitored by acoustic microphones or instrumented with accelerometers to acquire the overall vibration level.

Other experimental approaches in this field are based on the relief of the relative angular displacements of the gears by using encoders.[5,7] The above technique is generally used to analyse the errors and the discontinuities

[1]Department of Industrial Engineering, University of Naples Federico II, Naples, Italy
[2]Istituto Motori – Consiglio Nazionale delle Ricerche, Naples, Italy

Corresponding author:
Renato Brancati, Department of Industrial Engineering, University of Naples Federico II, Naples, Italy.
Email: renato.brancati@unina.it

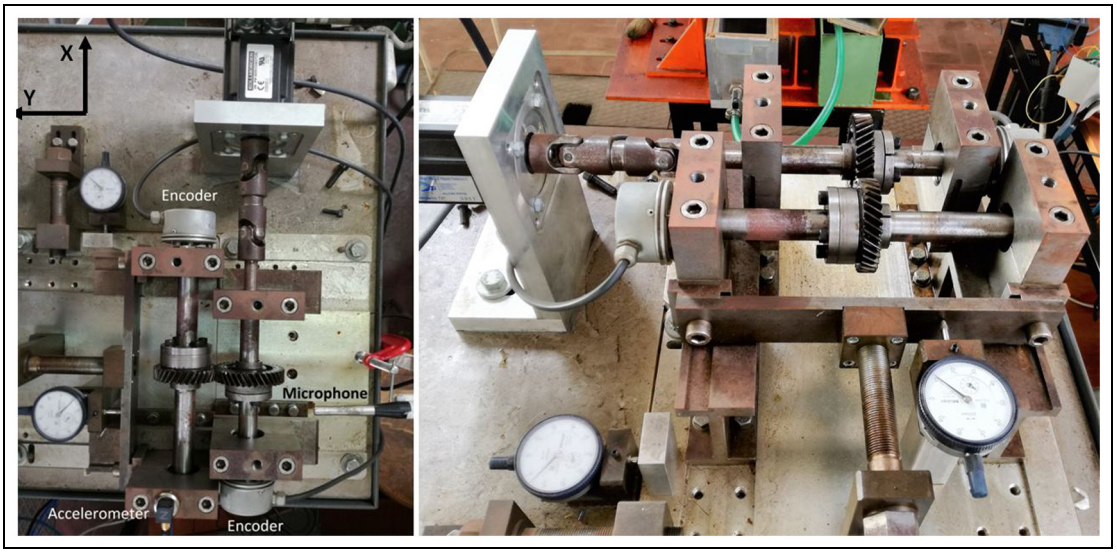

Figure 1. Instrumented rig.

in the contacts between the gear teeth or to acquire some kinematic quantities, such as the eccentricity of the wheels or the effective backlashes, which are useful to characterize the dynamic behaviour of the gears. This approach is suitable, in particular, to use in the diagnostics of gears.

Although in the literature many studies have considered the gear rattle generally forced by harmonic excitations, in the present paper a more realistic excitation of the multi-harmonic type is applied.[2]

In particular, the excitation consists of the sum of two harmonic components using the law of the pinion speed. Much attention was placed on determining a threshold for the onset of the gear rattle, in particular by comparing the acoustic noise radiated from a meshing gear pair with the data analysed in the frequency domain, which were acquired by an encoder-based methodology.

Another aspect examined in the present analysis considers the operative conditions of the gear pair in terms of the lubrication, and in particular the influence of the oil between the teeth during the impacts. This effect is well known in the literature,[7–11] because the presence of a lubricant in the impact phases acts as a damper by attenuating the gear rattle noise.

Experimental test rig

The experimental test rig consists of a helical spur gear, the pinion of which is driven by a speed-controlled brushless motor, with a maximum output torque of 2.2 N m. The motor speed controller enables an acceptable speed–time history to be found for the gear pair.

Apart from the negligible drag torque due to the bearings, no load is applied to the secondary shaft. Therefore, the test rig simulates 'idle' operating conditions.

The rig is instrumented to measure some mechanical quantities which are useful for performing a vibroacoustic analysis of the system. In particular, the measured parameters are as follows: the angular rotations of the gears by using encoders; the accelerations along three different directions from a triaxial accelerometer; the sound pressure level by employing microphones. The gear pair used for the present analysis is characterized by a transmission ratio $\varepsilon = z_2/z_1 = 33/37 = 0.89$. For the present tests, the distance between the axes was fixed at 65.5 mm. In this configuration, the measured angular backlash has a mean value of about 1.01×10^{-4} rad, with a periodic fluctuation ranging between a minimum value of 8.6×10^{-5} rad and a maximum of 1.17×10^{-4} rad, owing to assembly and manufacturing errors.

Vibrational and acoustic analyses were performed by integrating complementary instrumentation devices with the aim of correlating the causes and the effects, in order to determine the airborne or structure-borne noise transmission paths more effectively. A near-field acoustic sensor was used for complete scanning of the gear area to localize the noise sources satisfactorily. Figure 1 shows the test set-up.

The experimental equipment consists of the following:

(a) pressure transducers (PCB class 1 ICP microphone);
(b) a PCB triaxial accelerometer;
(c) two optical encoders;
(d) a multi-channel fast Fourier transform (FFT) analyser (LMS Siemens Scadas acquisition system);
(e) pre-processing software and post-processing software (LMS Test.Lab) for sound pressure level measurements.

Multi-harmonic excitation

The gear rattle noise is caused by oscillations of the angular speed induced by the irregularities of the engine torque. For this reason, as an excitation, a periodic speed law with two harmonic components was considered, which is given by

$$\Omega(t) = \Omega_m + A_1 \sin(2\pi f t) + A_2 \sin(4\pi f t) \quad (1)$$

where Ω_m is the mean value of the speed, A_1 and A_2 are the amplitudes of the speed fluctuation components and f is the fundamental frequency of the rattle cycle.

The experimental tests were carried out for three mean speed values: $\Omega_m = 500$ r/min, 600 r/min and 700 r/min. The fundamental component A_1 has an amplitude equal to 20% of the mean speed because it approximates, in practice, the speed irregularities of the automotive reciprocating engines; the amplitude of the second-order component A_2 ranges from 20% up to 100% of the A_1 component. The value of the fundamental frequency of rattle is $f = 5$ Hz for all the tests.

The experiments were performed under two lubrication conditions, namely dry lubrication and boundary lubrication. Dry lubrication was tested for use as a reference. In this case, no oil was used for the gears. The boundary lubrication consists of limited lubrication, which is characterized by a thin oil film on the flanks of each tooth, without any external oil feeding. The oil adopted for the tests has the following characteristics: SAE grade 80w90; test temperature, 20 °C; dynamic viscosity, approximately 0.35 Pa s.

Experimental results

In the following, some experimental results are reported, with reference to the various measurements techniques adopted for the investigation: angular motion measurements, vibration measurements and near-field and far-field acoustic measurements.

Angular motion measurements

The time histories of the relative angular motions of the gears are acquired by the use of two incremental encoders with a high resolution, fixed to each shaft. The resolution of the encoders is equal to 10,000 pulses/rev on each channel. By virtue of quadrature detection, each encoder provides therefore a resolution of 40,000 pulses/rev.

The speed law (1) was imposed at the pinion gear. In order to demonstrate that the desired speed law is correctly reproduced, Figure 2 shows the waterfall spectra, up to 40 Hz, measured by the pinion gear encoder. These spectra are for the case when the mean speed $\Omega_m = 500$ r/min and $A_1 = 100$ r/min, for various second-order harmonic amplitude values.

The transmission error (TE), which is defined as the relative angular motion $\Delta\theta(t)$, is measured by combining the two absolute rotations θ_1 and θ_2 of the gears according to

$$\Delta\theta(t) = \theta_1(t) - \theta_2(t)\frac{r_2}{r_1} = \theta_1(t) - \theta_2(t)\frac{z_2}{z_1}$$

where r_1 is the pitch radius of the pinion gear, r_2 is the pitch radius of the wheel gear, z_1 is the number of teeth on the pinion gear and z_2 is the number of teeth on the wheel gear.

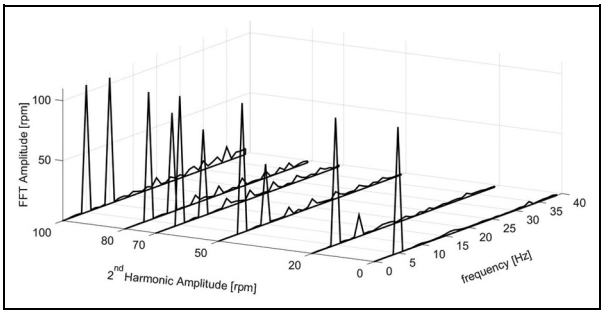

Figure 2. Harmonic components of the measured imposed motions (Ω_m = 500 r/min).
FFT: fast Fourier transform; rpm: r/min.

Figure 3 shows the TE and its FFT in the case of the pinion gear with a constant speed equal to 500 r/min. This case is reported as a reference to highlight the harmonic content of the pure rotations, without considering any fluctuations in the speed. The frequency components of the pinion gear rotations and the wheel gear rotations are evident in the diagrams. In fact, two major components can be observed, namely 8.33 Hz and 9.34 Hz, together with their ultra-harmonic components. In particular, the 9.34 Hz component appears to be more pronounced than the 8.33 Hz component, because of the presence of a tooth defect observed on the wheel gear; this is evidenced also by the spikes in the TE diagram.

Figure 4 shows the TEs and the FFTs for the cases of the first harmonic component equal to 100 r/min for a mean speed of 500 r/min, and for the second-order harmonic equal to 0 r/min, 50 r/min, 80 r/min and 100 r/min respectively. It is interesting to note that the FFT shows that the first harmonic of the relative motion initially increases and then decreases when the second-order excitation A_2 exceeds the value of 50 r/min. Moreover, the second-order component of the TE constantly increases when the second-order excitation increases.

Vibration measurements

Vibrational levels, which are acquired by using the triaxial accelerometer in the proximity of the driven-wheel shaft support (Figure 1), were investigated in

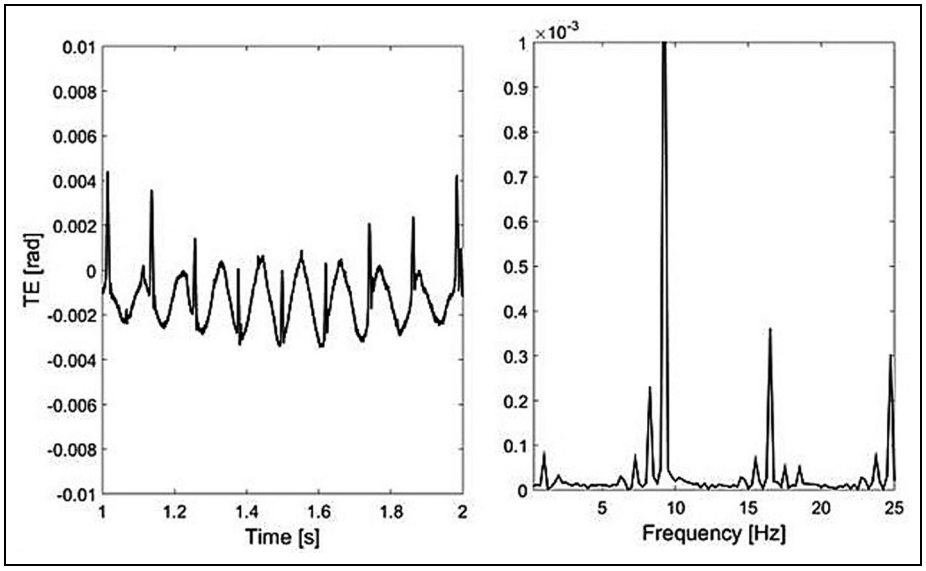

Figure 3. TE and FFT for the constant speed Ω_m = 500 r/min.
TE: transmission error.

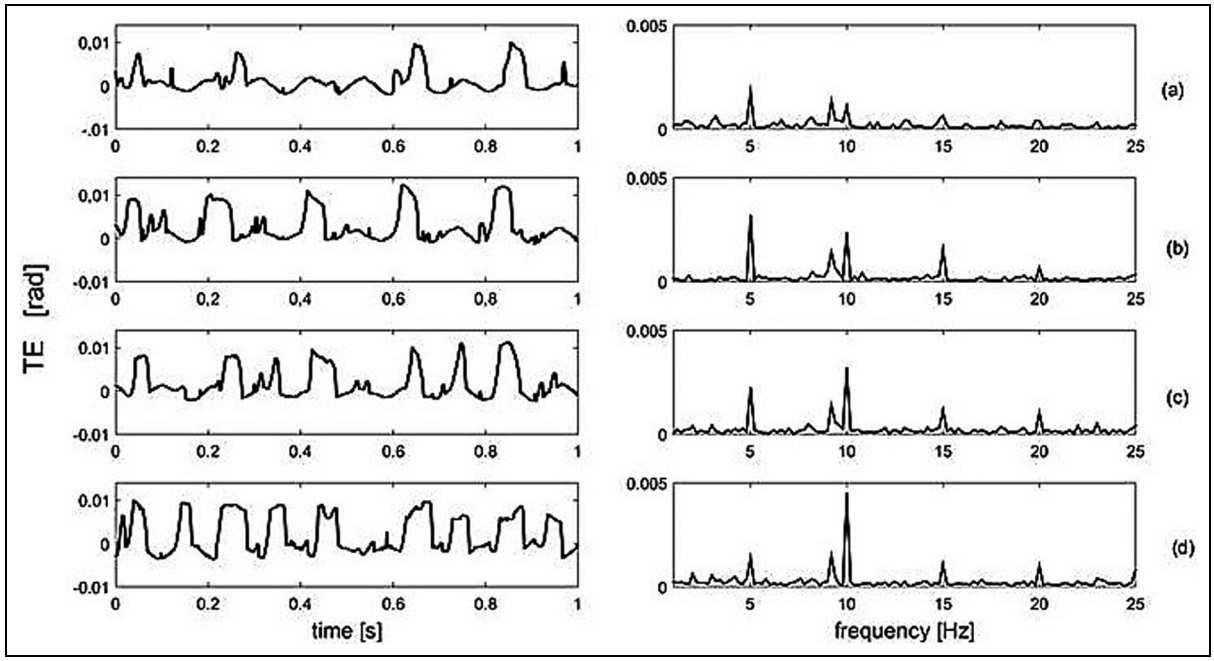

Figure 4. TE and FFT for Ω_m = 500 r/min and various A_2 amplitude values: (a) A_2 =0 r/min; (b) A_2 =50 r/min; (c) A_2 =80 r/min; (d) A_2 =100 r/min.
TE: transmission error.

terms of both the overall levels of acceleration and the spectral characteristics.

As appears evident from Figure 5, a generalized increase in the overall levels of vibrations can be noted as the second-order harmonic increases; the maximum vibration levels are along the y axis (the transverse axis).

It is also interesting to observe the positive effect of the oil lubrication which strongly reduces the overall vibration levels. Figure 6 shows, with reference to the case when Ω_m = 500 r/min, the x-axis, the y-axis and the z-axis vibration spectra as functions of the second-order harmonic of the excitation. It is confirmed that the vibrations along the y axis have a much larger amplitude than do the amplitudes for the other axes. Therefore, there is a negligible level of high-frequency vibrations along the z axis. The comparisons of spectra along the y axis clearly highlight the increase in the fundamental frequency, together with increases in its upper harmonics.

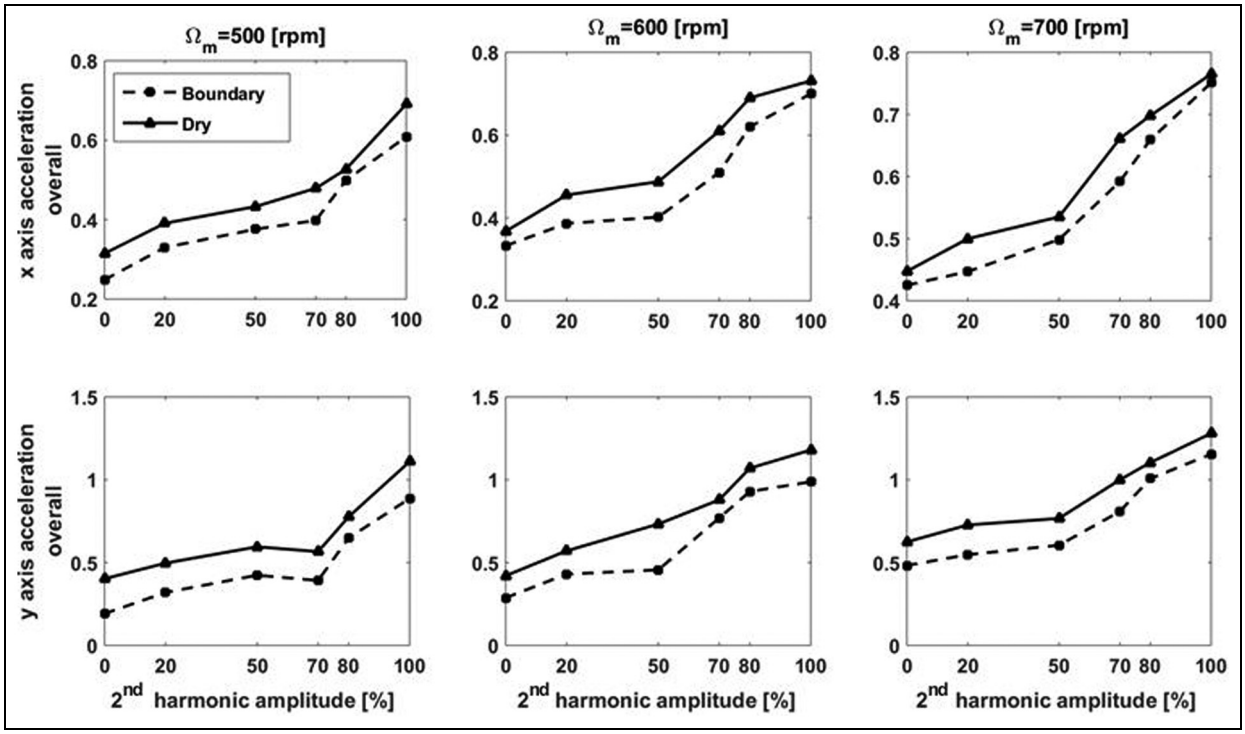

Figure 5. Overall vibrational levels along the *x* axis and the *y* axis as functions of the second-order harmonic A_2.
rpm: r/min.

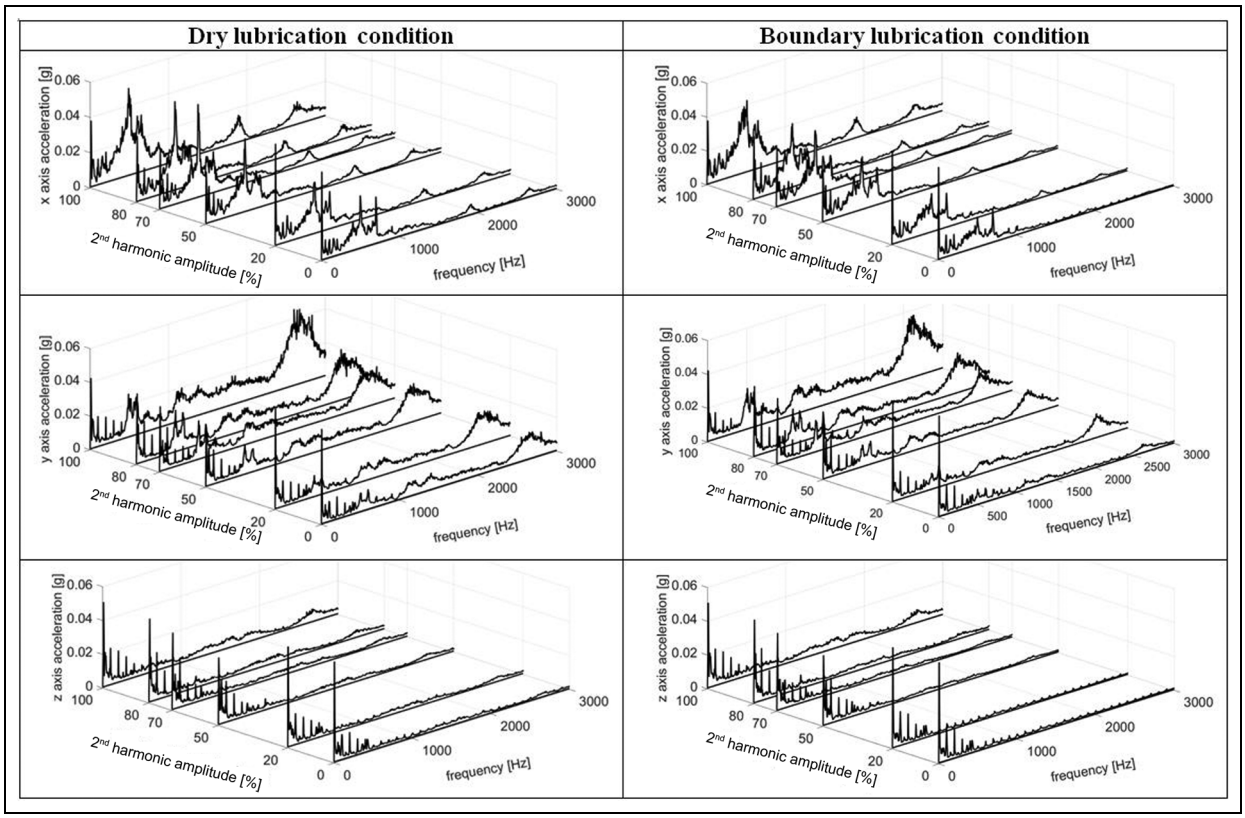

Figure 6. Vibration spectra as functions of the second-order harmonic A_2 (Ω_m = 500 r/min).

In the waterfall *x*-axis spectrum, a high level of vibrations can be observed for the frequencies near 600 Hz, which are due to the gear teeth meshing. With respect to the *y*-axis spectra, components are present at around 2500 Hz, which are caused by some structural resonances of the test rig.

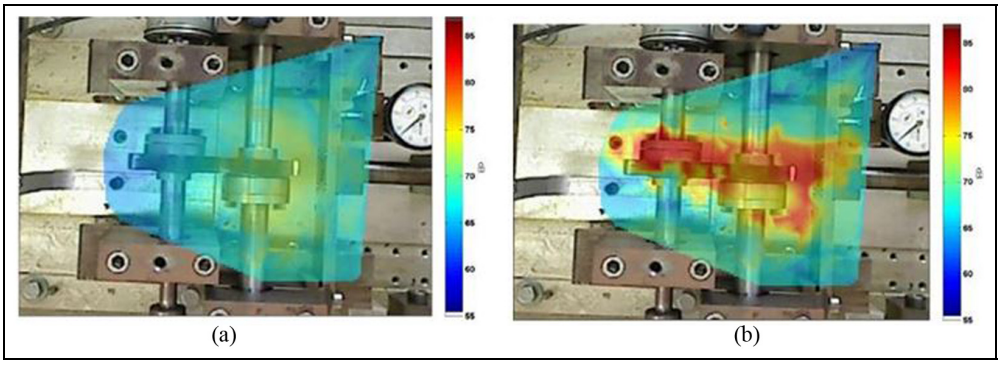

Figure 7. Direct mapping of the gear system for (a) the sound pressure and (b) the particle velocity for Ω_m = 500 r/min, A_1 =100 r/min and A_2 =70 r/min.

Near-field acoustic measurements

All the acoustic measurements are evaluated in terms of the relative values for the different operative conditions, more than in terms of the absolute values; this consideration is strictly related to the characteristics of the test environment (semi-reverberant) which cannot be assimilated to any of the standard acoustic test environments (i.e. anechoic, semi-anechoic or reverberant).

To justify this limitation, a particle velocity measurement technique was therefore introduced. Sound-pressure-based measurement methods and processing techniques often fail to provide appropriate results in such conditions owing to the high levels of background noise. Alternatively, maps of the particle velocity allow the acoustic excitations to be characterized across the system despite measurement in the harsh environment. More precisely, near-field experiments were performed by using novel instrumentation with the employment of a particle velocity sensor (Microflown). The Microflown acoustic sensor measures the velocity[12] of air 'particles' across two tiny resistive strips of platinum which are heated to about 300 °C. The temperature change due to a particular vibration close to the system under test is measured with a bridge circuit, which provides a signal proportional to the acoustic particle velocity. This particle velocity sensor is usually mounted together with a pressure microphone on a sound intensity *p–u* probe. When the particle velocity (sound) propagates orthogonally across the wires, it asymmetrically alters the temperature distribution around the resistors. The resulting resistance difference provides a broadband (0 Hz up to at least 20 kHz) linear signal that is proportional to the particle velocity up to sound levels of 135 dB. The reliability of measuring the sound level from particle velocity measurements close to rigid boundaries is well known, and also in the presence of other external sources; in fact, in near-field measurements, the contributions from other directions are strongly reduced.

The measurement procedure to acquire the data is based upon the scanning technique 'scan and paint'.[13]

The displacement of the Microflown *p–u* probe was recorded by a camera placed perpendicular to the test bench measurement area, so as to avoid any visual errors caused by the camera projection. A gear rattle scan was performed by moving the sensor close to the surface of the system. The camera recorded the displacement of the probe using discretization with about 150 points for each operating condition. Each scanning session lasted about 1 min. The experimental acquisitions were processed in the frequency range 20–5000 Hz. The results are combined with a background picture of the measured environment to obtain a visual representation which allows the noise source to be visualized and identified.

Figure 7 shows, for Ω_m =500 r/min, A_1 = 100 r/min and A_2 = 70 r/min, the normal particle velocity and the sound pressure maps in dry-lubrication conditions. The velocity vector was then measured using the particle velocity sensor, and the velocity surface distribution in the near field can be visualized as a contour map expressed in decibels (i.e. 5 $\times 10^{-8}$ m/s) to detect localization of the sound sources. Because the particle velocity is a vector, it is sensitive to the wave direction, and the *p–u* configuration provides a powerful combination for suppressing extraneous noise and reflections during its application.

As can be seen, by comparing the particle velocity and the pressure maps, no sound sources external to the gears can be identified on the pressure map. The reason is that the background noise, which is caused by sound sources distributed across the system, is masking the direct pressure emitted by specific areas of the vibrating structure, in contrast with the situation when viewing the particle velocity maps. It may be deduced that the gear system presents, in the evaluated frequency band, a most powerful excitation source which corresponds to the gears.

Figure 8(a) and (b) shows a comparison of the directy mapping, for Ω_m = 600 r/min, A_1 = 120 r/min and A_2 = 60 r/min, in the cases of dry lubrication and boundary lubrication respectively. It can be seen that the normal particle velocity maps for the two different

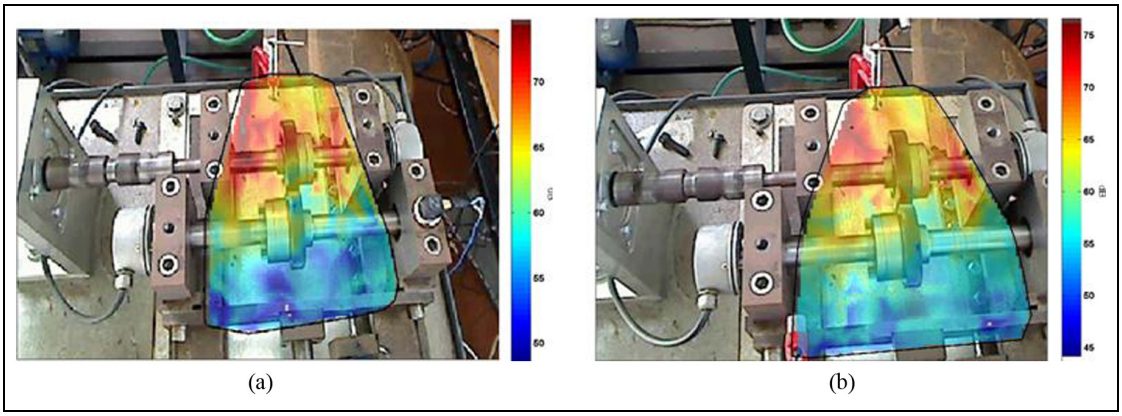

Figure 8. Direct mapping of the gear system for the particle velocity for Ω_m = 600 r/min, A_1 = 120 r/min and A_2 = 60 r/min in the cases of (a) dry lubrication and (b) boundary lubrication.

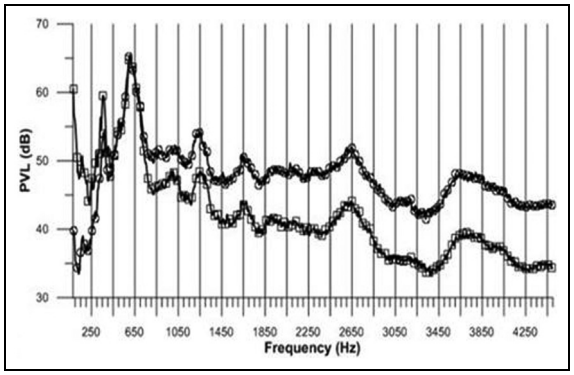

Figure 9. Comparison of the pressure velocity level spectra for Ω_m = 500 r/min, A_1 =100 r/min and A_2 = 70 r/min, with oil (open squares) and without oil (open circles).
PVL: pressure velocity level.

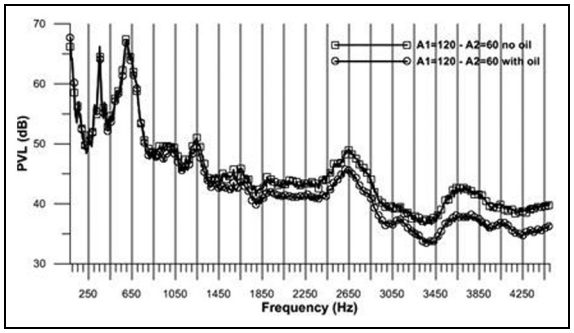

Figure 10. Comparison of the pressure velocity level spectra for Ω_m = 600 r/min, A_1 = 120 r/min and A_2 = 60 r/min, with oil (open circles) and without oil (open squares).
PVL: pressure velocity level.

lubrication conditions highlight the positive effect of lubrication.

The method to visualize and map the results in this way represents intuitive feedback from the measurements, allowing the noise sources across an unknown sound field to be easily localized.

Figure 9 and Figure 10 show comparisons of the pressure velocity spectra with the lubricant and without the lubricant respectively. For Figure 9, Ω_m = 500r/min, A_1 = 100 r/min and A_2 =70 r/min whereas, for Figure 10, Ω_m = 600r/min, A_1 = 120 r/min and A_2 = 60 r/min. The results reveal a noise source with two dominant peaks at about 300 Hz and 600 Hz, which represent the fundamental frequency and the second-order frequency respectively of the gear meshing. The presence of oil reduces the noise emitted by the system, achieving about 10 dB in some frequency bands.

Far-field acoustic measurements

In the present section, the results of the sound pressure analysis by employing microphones is reported. Time–frequency graphs in the dry-lubrication conditions are shown in Figure 11 and provide evidence of the stationary characteristics of the phenomena.

An analysis of the overall levels also shows, as previously verified for vibrational signals, an increase in the acoustic sound level as a function of the second-order harmonic amplitude. In Figure 12 the microphone overall levels for the three mean speed values of 500 r/min, 600 r/min and 700 r/min, for both lubrication operating conditions, are shown. The far-field measurements technique also reveals a sensitivity to the effect of the lubricant in reducing the gear rattle noise level.

In Figure 13 the waterfall spectra of acoustic signals are shown for the cases of dry lubrication and boundary lubrication respectively.

From an acoustic viewpoint, the frequency ranges of major interest are those shown in Figure 14, i.e. between 450 Hz and 750 Hz, where the amplitude of the signals is more evident. This figure shows the spectra of the microphone measurements for different values of the average speed and different amplitudes of the second harmonic, for dry-lubrication conditions. It can be seen that an increase in the A_2 component value causes an increase in the acoustic sound level.

As already stated with respect to the accelerometer results, the frequencies near 600 Hz are due to the meshing of gear teeth; in particular, they represent the second-order component of the meshing frequency.

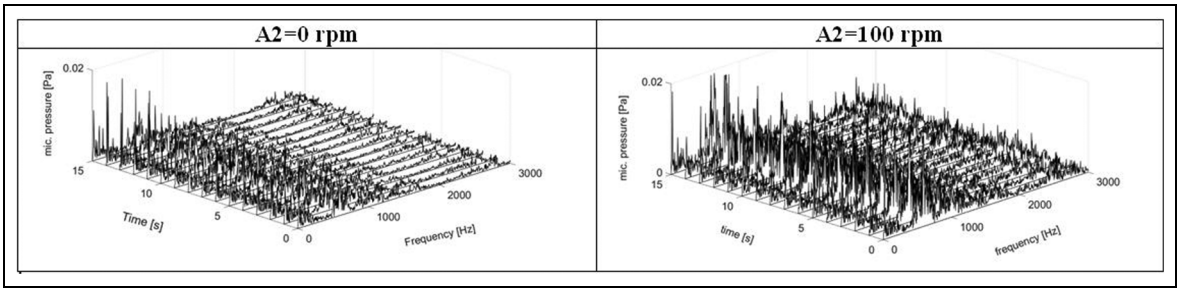

Figure 11. Acoustic waterfall spectra versus time (dry-lubrication conditions; Ω_m = 500 r/min; A_1 = 100 r/min).
mic.: microphone; rpm: r/min.

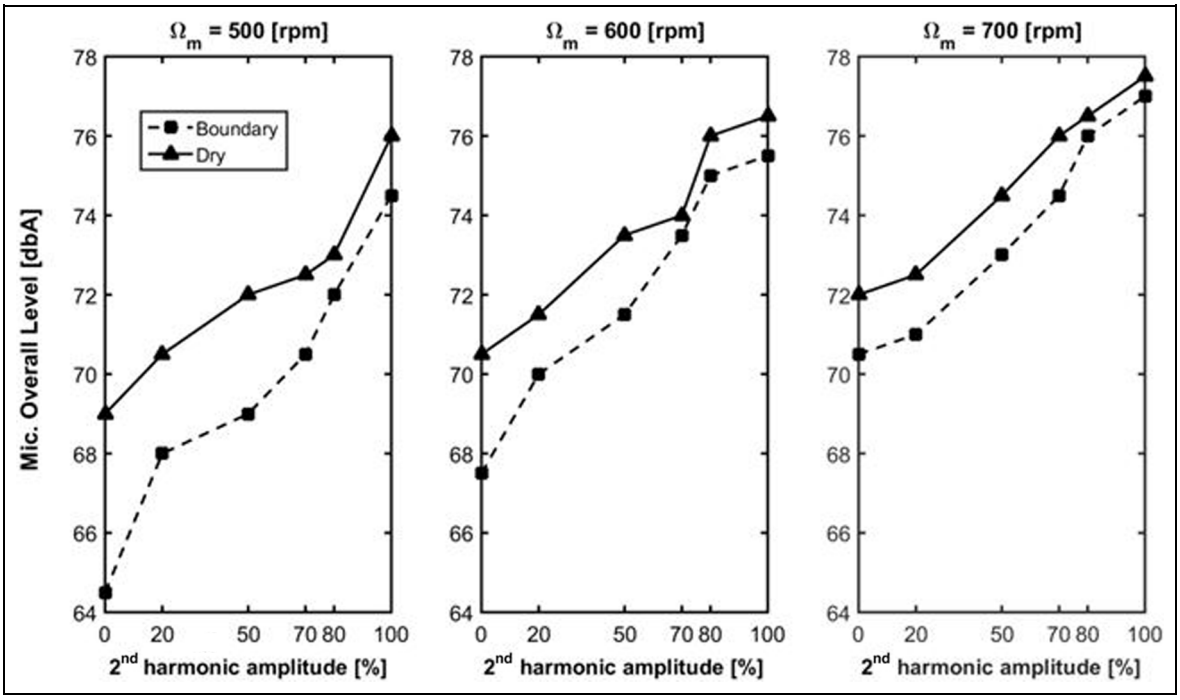

Figure 12. Overall vibrational levels.
Mic.: microphone; rpm: r/min.

Figure 15 shows the sound level in the above frequency ranges for the two mean speed values of 500 r/min and 700 r/min, where the effect of oil can be observed by comparing the diagrams for the different lubrication conditions.

Gear rattle index

A *gear rattle index* (IGR) has been defined in previous work and is adopted in order to compare and discriminate, in an objective way, between different vibro-acoustic behaviours caused by different excitations, and also by different lubrication conditions. The IGR, which is referred to as the relative angular motion $\Delta\theta$ of the gears, is defined as the value of the integral[7,14] between 20 Hz and 5000 Hz according to

$$\mathrm{IGR} = \int_{20\ \mathrm{Hz}}^{5000\ \mathrm{Hz}} |\Delta\theta(\omega)|\ \mathrm{d}\omega \qquad (2)$$

In the present analysis the index was evaluated for the experimental signals from the encoders, for the spectra from the accelerometer measurements and for the spectra from the acoustic sound measurements.

Figures 16, 17 and 18 show the values of the IGR calculated with reference to the above-mentioned experimental measurements.

It should be noted that the IGR metric gives reliable information with regard to the vibro-acoustic behaviour independently of the adopted measurement methodology. In fact, the index gives, qualitatively, analogous results of the analysis performed by the encoders, i.e. it increases with increasing A_2 excitation component. Moreover, the index includes the positive effect due to the oil in reducing the rattle.

Conclusion

In this paper, an experimental analysis of the gear rattle phenomenon was presented using a correlation between

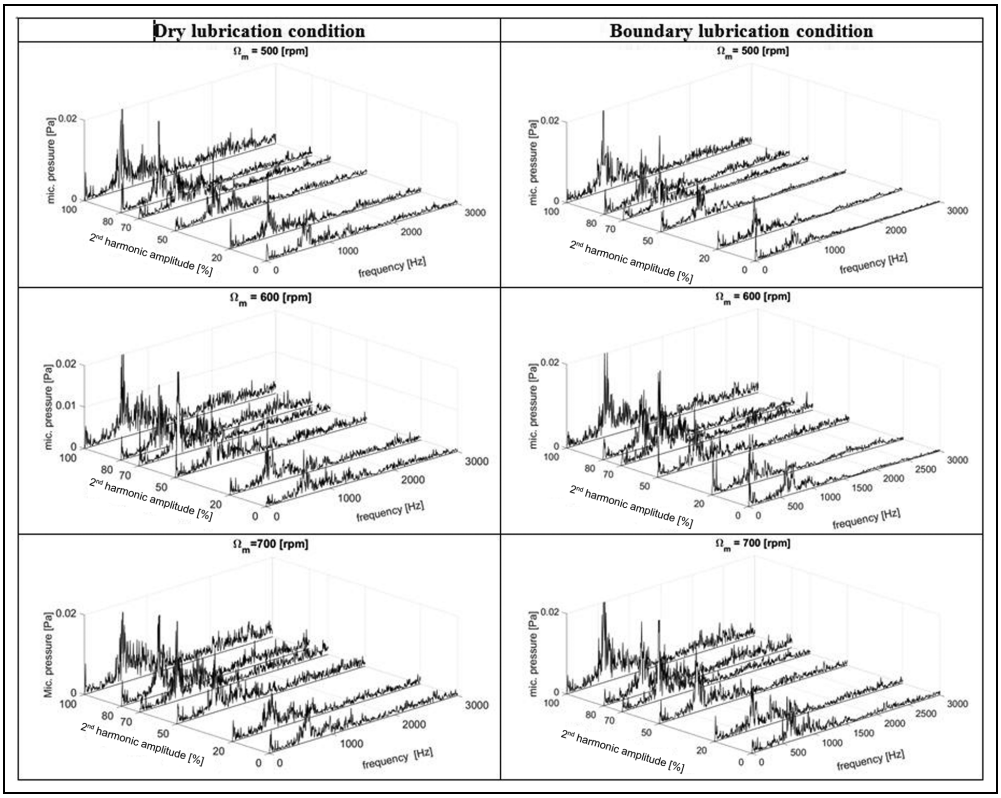

Figure 13. Waterfall spectra of the acoustic signals.
mic.: microphone; rpm: r/min.

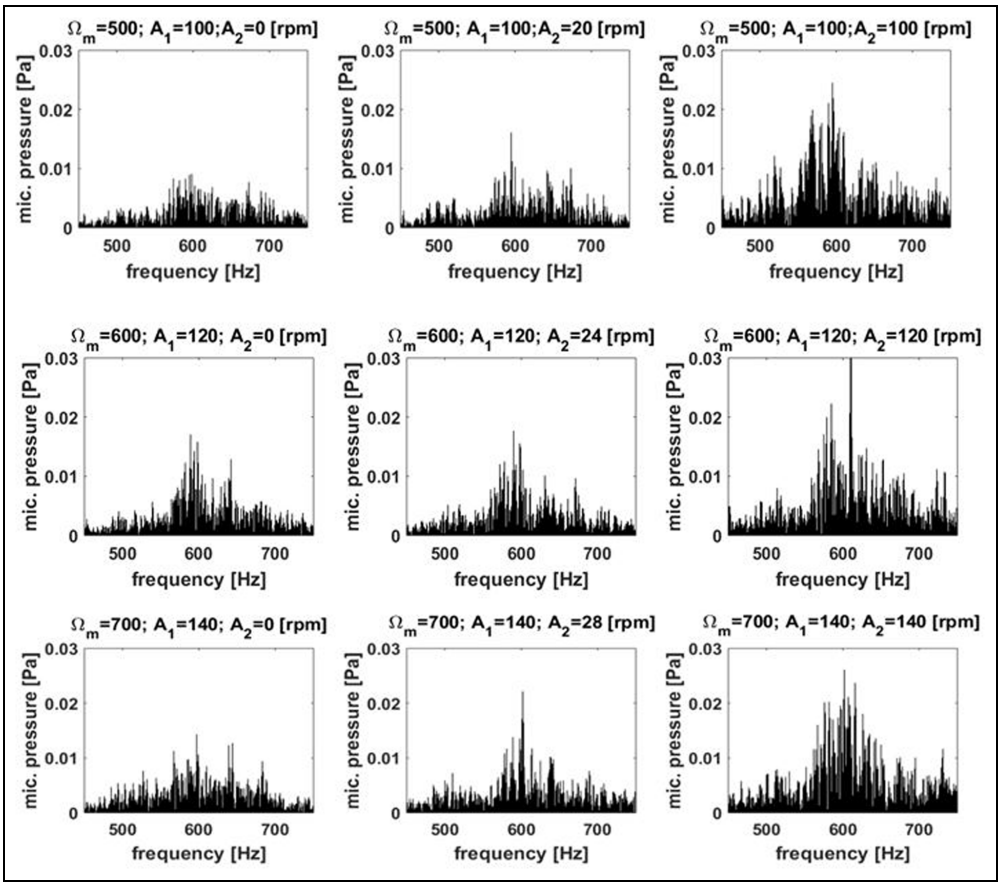

Figure 14. Acoustic sound level spectra for the 450–750 Hz range.
mic.: microphone; rpm: r/min.

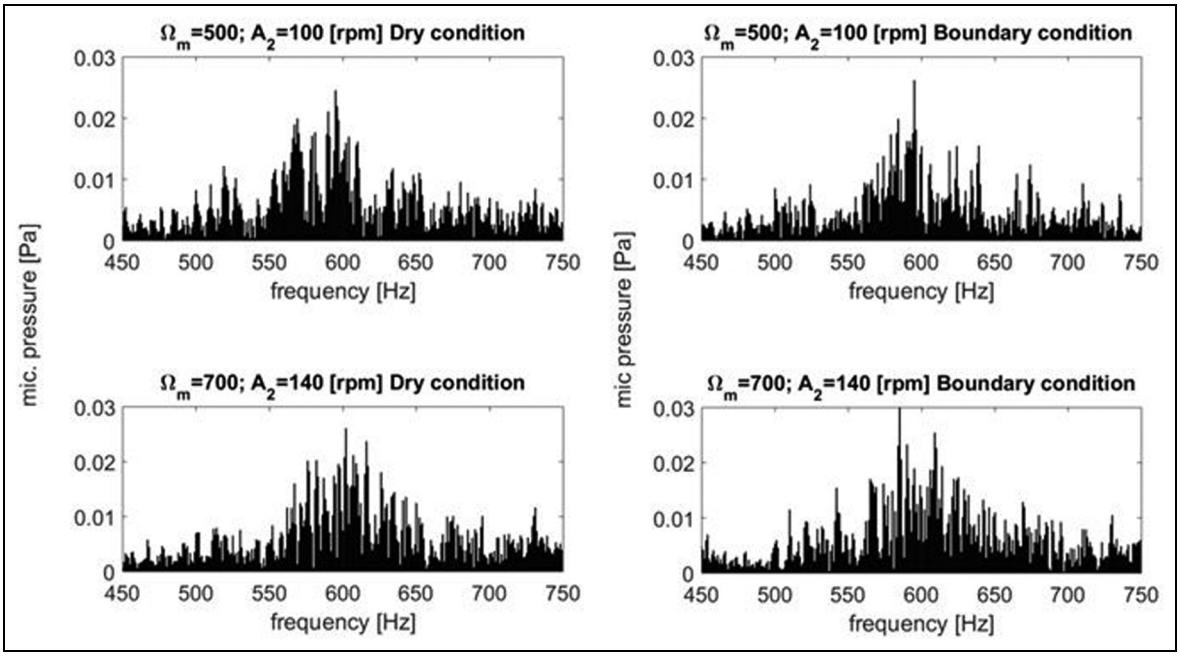

Figure 15. Sound spectra comparisons for two lubrication conditions.
mic.: microphone; rpm: r/min.

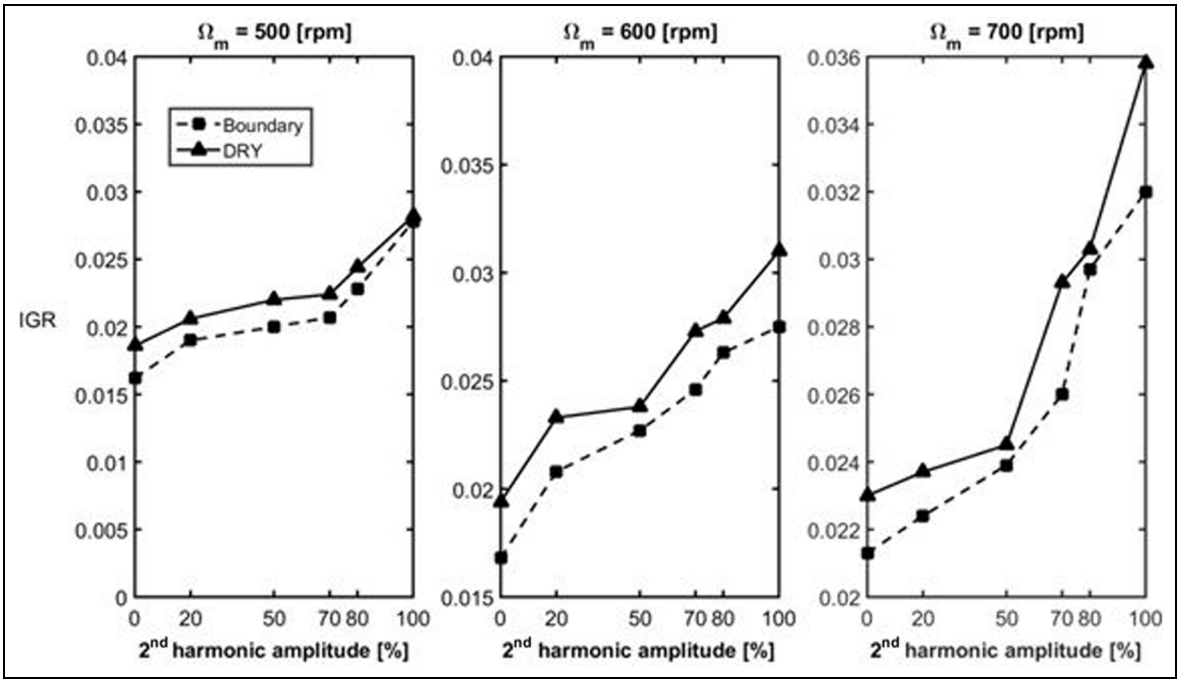

Figure 16. IGR for the encoder measurements.
IGR: gear rattle index; rpm: r/min.

different measurement methodologies for the acoustic sound emissions, the levels of vibrations and the angular motions of the gears.

The study was performed on a dedicated test set-up where the rattle phenomenon was induced through multi-harmonic excitation with two components, for which the second-order component amplitude was varied in particular.

The acquisition of the sound pressure level from acoustic microphones was supported by an investigation with a *p–v* sound intensity probe, for correct evaluation of the near-field acoustic sources.The vibro-acoustic analysis showed notable results about the correlation with the encoder-based methodology, which enables an accurate analysis of the tooth contacts and impacts occurring during the rattle to be made. From

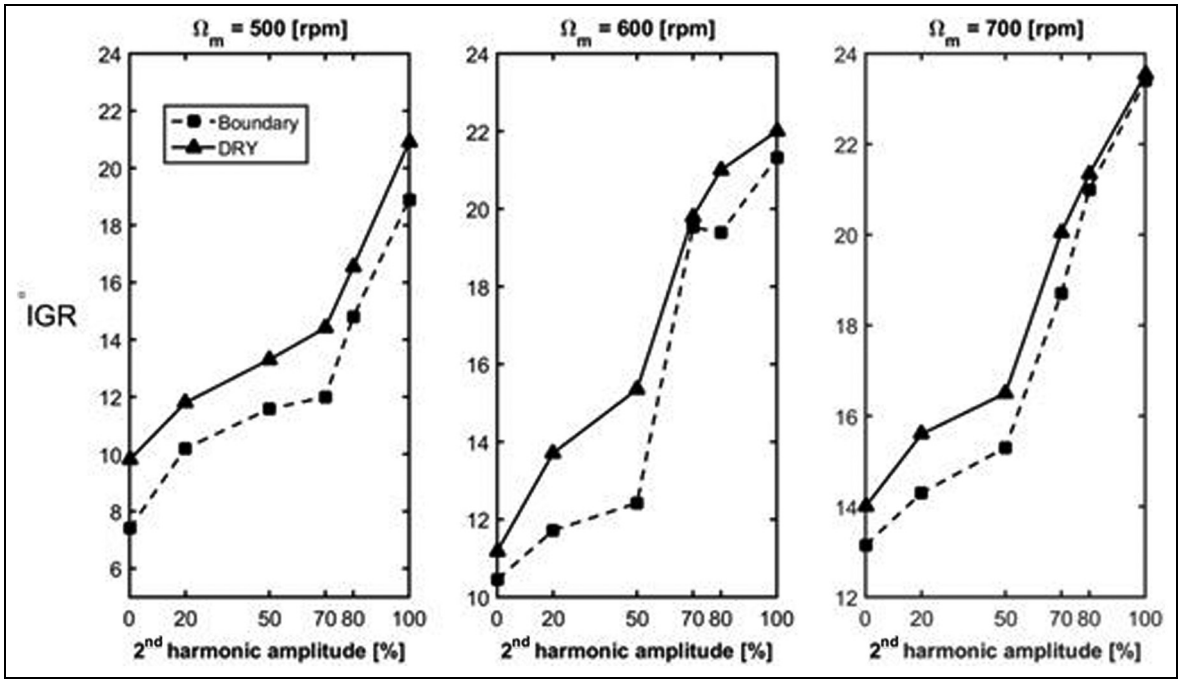

Figure 17. IGR for the accelerometer measurementss along the *x* axis.
IGR: gear rattle index; rpm: r/min.

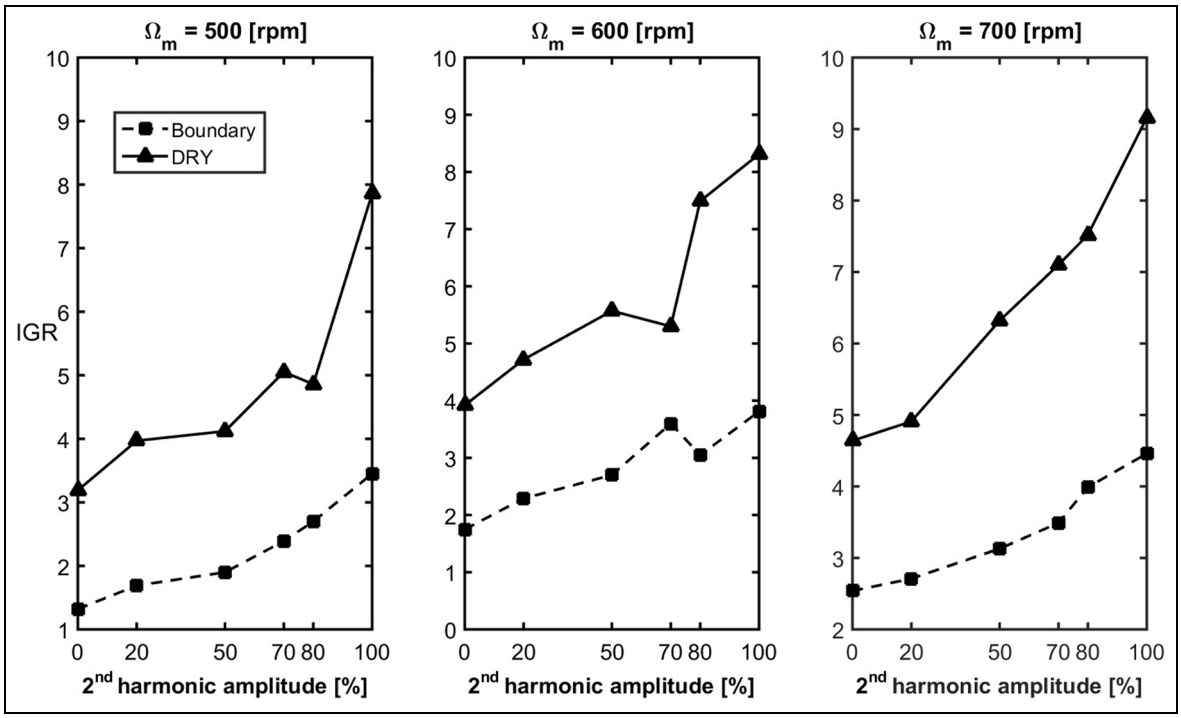

Figure 18. IGR for the acoustic sound measurements.
IGR: gear rattle index; rpm: r/min.

an acoustic viewpoint, the analysis not only demonstrates that the lubricant always plays a positive role in the reduction of the rattle noise but also shows that the presence of the second harmonic in the excitation still causes an increase in the acoustic noise level. In particular, the microphone measurements highlighted that the second harmonic of the excitation amplifies the frequencies around 600 Hz (near to the second order of gear meshing). The results of the *p–v* acoustic investigation instead reveal a dominant noise source in the frequency range 250–750 Hz, with two dominant peaks corresponding to about 300 Hz and 600 Hz, which

represent the gear-meshing frequency and its second-order component respectively.

The qualitative good agreement between the different methodologies was confirmed also by a performance index developed by the present authors on the basis of the harmonic analysis of data.

Although each measurement technique provides specific information on the behaviour of the gears, the present investigation makes it clear that, depending on the particular needs of the researcher, it is possible to achieve similar results, from a qualitative point of view, using any one of the proposed methodologies.

Acknowledgements

The authors thank Gennaro Stingo and Giuseppe Iovino of the Department of Industrial Engineering, University of Naples Federico II, for their fundamental technical support during the tuning stages of the test rig.

Declaration of conflicting interests

The author(s) declared no potential conflicts of interest with respect to the research, authorship, and/or publication of this article.

Funding

The author(s) disclosed receipt of the following financial support for the research, authorship, and/or publication of this article: This research received no specific grant from any funding agency in the public, commercial or not-for-profit sectors.

References

1. Wang Y, Manoj R and Zhao W J. Gear rattle modeling and analysis for automotive manual transmissions. *Proc IMechE Part D: J Automobile Engineering* 2001; 215(2): 241–258.
2. Barthod M, Hayne B, Tebec JL et al. Experimental study of gear rattle excited by a multi- harmonic excitation. *Appl Acoust* 2007; 68(9): 1003–1025.
3. Dogan S N, Ryborz J and Bertsche B. Design of low-noise manual automotive transmissions. *Proc IMechE Part K: J Multi-body Dynamics* 2006; 220(2): 79–95.
4. Brancati R, Rocca E, Savino S et al. Experimental analysis of the relative motion of a gear pair under rattle conditions induced by multi-harmonic excitation. In: *World congress on engineering*, London, UK, 1–3 July 2015, pp. 1016–1021. London: IAENG.
5. Younes K, Rigaud E, Perret-Liaudet J et al. Experimental and numerical analysis of automotive gearbox rattle noise. *J Sound Vibr* 2012; 331(13): 3144–3157.
6. Brancati R, Montanaro U, Rocca E et al. Analysis of bifurcations, rattle and chaos in a gear transmission system. *Int Rev Mech Engng* 2013; 7(4): 583–591.
7. Rocca E and Russo R. Theoretical and experimental investigation into the influence of the periodic backlash fluctuations on the gear rattle. *J Sound Vibr* 2011; 330(20): 4738–4752.
8. Brancati R, Rocca E and Russo R. A gear rattle model accounting for oil squeeze between the meshing gear teeth. *Proc IMechE Part D: J Automobile Engineering* 2005; 219(9): 1075–1083.
9. De la Cruz M, Theodossiades S and Rahnejat H. An investigation of manual transmission drive rattle. *Proc IMechE Part K: J Multi-body Dynamics* 2010; 224(2): 167–181.
10. Theodossiades S, De la Cruz M and Rahnejat H. Prediction of airborne radiated noise from lightly loaded lubricated meshing gear teeth. *Appl Acoust* 2015; 100: 79–86.
11. Brancati R, Rocca E and Russo R. An analysis of the automotive driveline dynamic behaviour focusing on the influence of the oil squeeze effect on the idle rattle phenomenon. *J Sound Vibr* 2007; 303(3–5): 858–872.
12. Siano D, Viscardi M and Panza A. Experimental acoustic measurements in far field and near field conditions: characterization of a beauty engine cover. In: *12th international conference on fluid mechanics and aerodynamics and 12th international conference on heat transfer, thermal engineering and environment*, Geneva, Switzerland, 29–31 December 2014, pp. 50–57. Geneva: WSEAS.
13. Siano D, Viscardi M and Aiello R. Experimental and numerical validation of an automotive subsystem through the employment of FEM/BEM approaches. *Energy Procedia* 2015; 82: 67–74.
14. Brancati R., Rocca E., Lauria D. Feasibility study of the Hilbert transform in detecting the gear rattle phenomenon of automotive transmissions Journal of Vibration and Control prepublished February 1, 2017 DOI: 10.1177/1077546316689745

Appendix 1

Notation

A_i	amplitudes of the speed fluctuation components ($i = 1, 2$)
f	fundamental frequency of the rattle cycle
r_1	pitch radius of the pinion gear
r_2	pitch radius of the wheel gear
z_1	number of teeth on the pinion gear
z_2	number of teeth on the wheel gear
$\Delta\theta$	transmission error
ε	transmission ratio
θ_i	absolute rotations of the gears ($i = 1, 2$)
Ω	angular speed
Ω_m	mean value of the angular speed